



## Large and realistic models of amorphous silicon

Dale Igram<sup>a</sup>, Bishal Bhattarai<sup>a</sup>, Parthapratim Biswas<sup>b</sup>, D.A. Drabold<sup>c,\*</sup>

<sup>a</sup> Department of Physics and Astronomy, Condensed Matter and Surface Science Program (CMSS), Ohio University, Athens, OH 45701, USA

<sup>b</sup> Department of Physics and Astronomy, The University of Southern Mississippi, Hattiesburg, MS 39406, USA

<sup>c</sup> Department of Physics and Astronomy, Nanoscale and Quantum Phenomena Institute (NQPI), Ohio University, Athens, OH 45701, USA



### ARTICLE INFO

#### Keywords:

*Ab initio*

Reverse monte carlo

Inverse modeling

Amorphous silicon

Phonons

Specific heat

### ABSTRACT

Amorphous silicon (*a*-Si) models are analyzed for structural, electronic and vibrational characteristics. Several models of various sizes have been computationally fabricated for this analysis. It is shown that a recently developed structural modeling algorithm known as force-enhanced atomic refinement (FEAR) provides results in agreement with experimental neutron and X-ray diffraction data while producing a total energy below conventional schemes. We also show that a large model ( $\sim 500$  atoms) and a complete basis is necessary to properly describe vibrational and thermal properties. We compute the density for *a*-Si, and compare with experimental results.

### 1. Introduction

Amorphous silicon (*a*-Si) and its hydrogenated counterpart (*a*-Si:H) continue to play an important role in technological applications, such as thin-film transistors, active-matrix displays, image-sensor arrays, multi-junction solar cells, multilayer color detectors, and thin-film position detectors [1]. While a number of traditional methods, based on Monte Carlo and molecular-dynamics simulations, were developed in the past decades by directly employing classical or quantum-mechanical force fields – from the event-based Wooten-Winer-Weaire (WWW) [2, 3] bond-switching algorithm and the activation-relaxation technique (ART) [4, 5] to the conventional melt-quench (MQ) molecular-dynamics simulations [6–11] – none of the methods utilize prior knowledge or experimental information in the simulation of atomistic models of complex materials. It is now widely accepted that dynamical methods perform rather poorly to generate high-quality (i.e., defect-free) continuous-random-network (CRN) models of amorphous silicon by producing too many coordination defects (e.g., 3- and 5-fold coordinated atoms) in the networks. While the WWW algorithm and the ART can satisfactorily address this problem by producing 100% defect-free CRN models of *a*-Si, a direct generalization of the WWW algorithm for multicomponent systems is highly nontrivial in the absence of sufficient information on the bonding environment of the atoms. Likewise, the ART requires a detailed knowledge of the local minima and the saddle points on a given potential-energy surface in order to determine suitable low-lying minima that correspond to defect-free CRN models of amorphous silicon. On the other hand, the availability of high-precision experimental data from diffraction, infrared (IR), and nuclear magnetic

resonance (NMR) measurements provide unique opportunities to develop methods, based on information paradigm, where one can directly incorporate experimental data in simulation methodologies. The reverse Monte Carlo (RMC) method [12–15] is an archetypal example of this approach, where one attempts to determine the structure of complex disordered/amorphous solids by inverting experimental diffraction data. Despite its simplicity and elegance, the method produces unphysical structures using diffraction data only. While inclusion of appropriate geometrical/structural constraints can ameliorate the problem, the generation of high-quality models of *a*-Si, using constrained RMC simulations, has been proved to be a rather difficult optimization problem and satisfactory RMC models of *a*-Si have not been reported in the literature to our knowledge. The difficulty associated with the inversion of diffraction data using RMC simulations has led to the development of a number of hybrid approaches in the past decade [16, 17]. Hybrid approaches retain the spirit of the RMC philosophy as far as the use of experimental data in simulations is concerned but go beyond RMC by using an extended penalty function, which involves total energy and forces from appropriate classical/quantum-mechanical force fields, in addition to few structural or geometrical constraints. The experimentally constrained molecular relaxation [18, 19] (ECMR), the first-principle assisted structural solutions [20] (FPASS), and the recently developed force-enhanced atomic relaxation [21–24] (FEAR) are a few examples of hybrid approaches, which have successfully incorporated experimental information in atomistic simulations to determine structures consistent with both theory and experiments. Recently, the FEAR has been applied successfully to simulate amorphous carbon (*a*-C) [24]. This is particularly notable as the latter can exist in a

\* Corresponding author.

E-mail addresses: [di994313@ohio.edu](mailto:di994313@ohio.edu) (D. Igram), [bb248213@ohio.edu](mailto:bb248213@ohio.edu) (B. Bhattarai), [partha.biswas@usm.edu](mailto:partha.biswas@usm.edu) (P. Biswas), [drabold@ohio.edu](mailto:drabold@ohio.edu) (D.A. Drabold).

variety of complex carbon bonding environment, which makes it very difficult to produce *a*-C from *ab initio* molecular-dynamics simulations due to the lack of *glassy* behavior and the WWW bond-switching algorithm in the absence of prior knowledge of the bonding states of C atoms in *a*-C (e.g., the ratio of  $sp^2$ - versus  $sp^3$ -bonded C atoms with a varying mass density). In this paper, we show that the information-based FEAR approach can be employed effectively to large-scale simulations of *a*-Si consisting of 1000 atoms. The resulting models have been found to exhibit superior structural, electronic, and vibrational properties of *a*-Si as far as the existing RMC and *ab initio* MD models are concerned in the literature.

The rest of the paper is as follows. In Section 2, we discuss the computational methodology associated with the generation of CRN models using the FEAR method. This is followed by the validation of the properties of the FEAR models with particular emphasis on the structural, electronic, vibrational, and thermal properties in Section 3. Section 4 presents the conclusions of our work.

## 2. Methodology and models

For this study, three model sizes (216, 512 and 1024 atoms) were implemented with FEAR and compared with experimental data. Several algorithms and codes were utilized for the preparation of the models; namely, FEAR [21–23], RMCProfile [27], SIESTA [28] and VASP [29–31].

A random starting structure was constructed for each of the models and was refined by fitting to the experimental pair correlation functions  $g(r)$  and/or the static structure factor  $S(q)$  by employing RMCProfile. The refined structure is relaxed using conjugate gradient (CG) in SIESTA. The relaxed-refined structure is then refined by RMCProfile. This cyclic process is repeated until convergence is achieved (in this work, each FEAR step is defined by  $\sim 100$  RMC accepted moves followed by 1 CG step, and a total of 6,000 FEAR steps were sufficient for a reasonable model of *a*-Si). For completeness the converged structure is then fully relaxed by VASP (plane wave LDA).

The partial refinement steps in RMCProfile were carried out with a minimum distance between atoms of 2.10 Å and maximum move distance of 0.15 Å–0.35 Å. The partial relaxation steps utilized SIESTA with a single- $\zeta$  basis set, Harris functional at constant volume, exchange-correlation functional with local-density approximation (LDA), periodic boundary conditions and a single relaxation step. The final relaxation step employed VASP with a plane-wave basis set, plane-wave cutoff of 350–450 eV, energy difference criteria of  $10^{-4} - 10^{-5}$ . The fully relaxed calculations were performed for  $\Gamma(\vec{k} = 0)$ . For all the FEAR models, we have used structure factor data from Laaziri et al. [25] for RMC refinement.

The three FEAR models and 216 MQ model have a number density of about 0.05005 atoms / Å<sup>3</sup>, which is associated with atomic density of 2.33 g/cm<sup>3</sup> (for details Table 1). The 216 MQ model was fabricated by taking a set of random coordinates and equilibrating these coordinates at 3000 K for 6 ps, followed by cooling from 3000 K to 300 K within 9 ps, then equilibration at 300 K for 4.5 ps, and a full relaxation at 300 K. The MQ calculations were performed with a step size of 1.5 fs. These are typical simulation times used to prepare accurate *ab initio* models for *a*-Si.<sup>1</sup>

We have also considered two large (4096 atoms and 10,000 atoms) WWW [2, 3] models in our comparison. These two WWW models were relaxed using SIESTA with a single- $\zeta$  basis set, LDA at constant volume utilizing Harris functional.<sup>2</sup>

<sup>1</sup> It is worth noting that MQ is not a unique process, and it has recently been shown that very slow quenches of liquid silicon can lead to models approaching WWW quality, contrary to the conventional view that MQ only works for glass formers. These are very extended simulations however, and do not seem to be a very efficient way (FEAR is an efficient method, and the models reported here required only 6,000 force calls) to model non-glass forming materials [32–34].

## 3. Results

### 3.1. Structural properties

A comparison of structure factors for the six models 216 MQ, 216 FEAR, 512 FEAR, 1024 FEAR, 4096 WWW and 10,000 WWW models with respect to experiment [25, 26] is shown in Fig. 1. From Fig. 1 (left panel) we can clearly observe that these models of up to 512 atoms is insufficient to resolve the first peak occurring at low  $q$ . In contrast, the 1024 FEAR model does well even in comparison to much larger models as seen in Fig. 1 (right panel). This is also indicated in the real space information  $g(r)$  (Fig. 2), where we observe that 10,000 WWW model is slightly shifted as compared to the experiment [25] for the first and second neighbors peak. We report the details of our simulation and important observables in Table 1.

From Table 1, we observe that there are some defects in our models. These structural defects arise due to a small fraction ( $\sim 5\%$ ) of over-coordinated and under-coordinated atoms. This explains the fact that all of our models have coordination value slightly above perfect four-fold coordination. Experimentally, it is also observed that *a*-Si does not possess a perfect four fold coordination [25, 26]. Our final models obtained after relaxation attain energies (eV/atom) equal or less than models obtained from MQ.

We further show our plots of bond-angle distribution in Fig. 2 (right panel) to attest accuracy of FEAR models. As seen in Fig. 2 the peak of the bond angle is close to the value of tetrahedral angle 109.47°. Similarly, from ring statistics (Fig. 3) we observe that these *a*-Si networks mostly prefer a ring size of 5, 6, 7. Small rings (mostly 3-membered rings) are responsible for a unrealistic peak seen in unconstrained RMC [21] at an angle around  $\sim 60^\circ$ . Opletal et al. have proposed use of a constraint for removal of these highly constrained 3 membered rings in their several works [16, 35]. FEAR method which incorporates accurate *ab initio* interaction enables us to remove these high energy structures without satisfying an extra criterion.

### 3.2. Electronic properties

Electronic properties such as electronic density of states (EDOS) reveal crucial information regarding accuracy of models. In particular, Prasai et al. and others [38, 39] have used electronic information to aid in modeling amorphous system. Conversely, EDOS obtained for our models validate accuracy of our models. We have shown our plot of four models in Fig. 4. We have also studied the localization of electronic states by plotting inverse participation ratio (IPR) in conjunction with EDOS. We observe both plots with same qualitative resemblance with few localized states appearing near the Fermi energy ( $E_F = 0$ ). These localized states arise due to the defects in the model (3-fold and 5-fold atoms).

We compare our large model of 4096 atoms along with our FEAR models. Due to gigantic size of this model, we have used Harris Functional and single- $\zeta$  basis set to evaluate the electronic density of states of these models. To our knowledge this is first time reporting of an *ab initio* based EDOS of *a*-Si models this big. Drabold et al. have previously carried out an extensive research regarding the exponential tail (valance and conduction) observed in amorphous silicon [40–42]. We report our result of EDOS for these models in Fig. 5. We observe that a 216 atom model gives us a very crude representation of these tails (valance and conduction). Meanwhile, FEAR models 512 and 1024 compare well with the large WWW models. Fedders et al. [43] have revealed that the valance tail prefers short bonds while the conduction tail prefers long bonds.

<sup>2</sup> We minimized our 4096 WWW model to have forces less than 0.01 eV/Å and for the 10,000 WWW model after  $\sim 100$  CG steps, RMS force of 0.024 eV/Å was obtained.

**Table 1**

Nomenclature and details of our models: Length of the cubic box ( $L$ ), position of first ( $r_1$ ) and second ( $r_2$ ) peak of RDF, Average coordination number ( $n$ ), percentage of 3-fold, 4-fold and 5-fold coordinated atoms, Free Energy per atom of the final VASP relaxed models ( $E_0$ ).

Model	$L$ (Å)	$r_1$ (Å)	$r_2$ (Å)	$n$	3-fold %	4-fold %	5-fold%	$E_0$ (eV/atom)
216MQ	16.28	2.36	3.81	4.083	0.93	87.03	11.57	0.000
216FEAR	16.28	2.36	3.81	4.028	1.39	94.44	4.17	-0.002
512FEAR	21.71	2.35	3.82	4.008	1.17	95.90	2.73	-0.044
1024FEAR	27.35	2.36	3.79	4.018	2.34	94.53	3.13	-0.035
4096WWW	43.42	2.36	3.78	4.004	0.05	99.46	0.49	-
10,000WWW	57.32	2.31	3.69	4.014	0.04	98.60	1.30	-

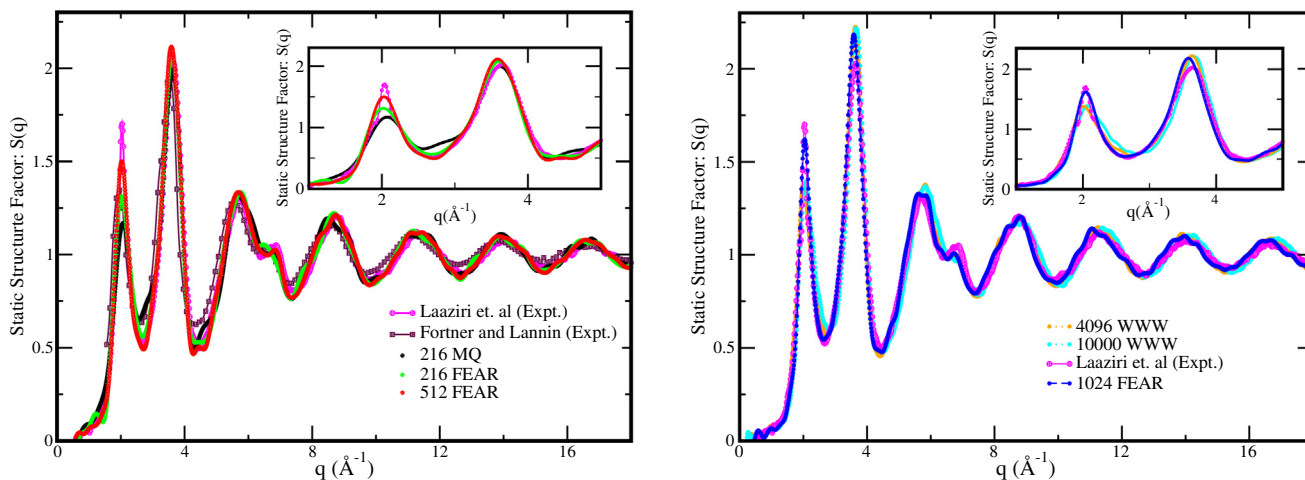


Fig. 1. Structure factor for different models and their comparison with experiments. [25, 26] Inset: Plot of low  $q$  region of structure factor.

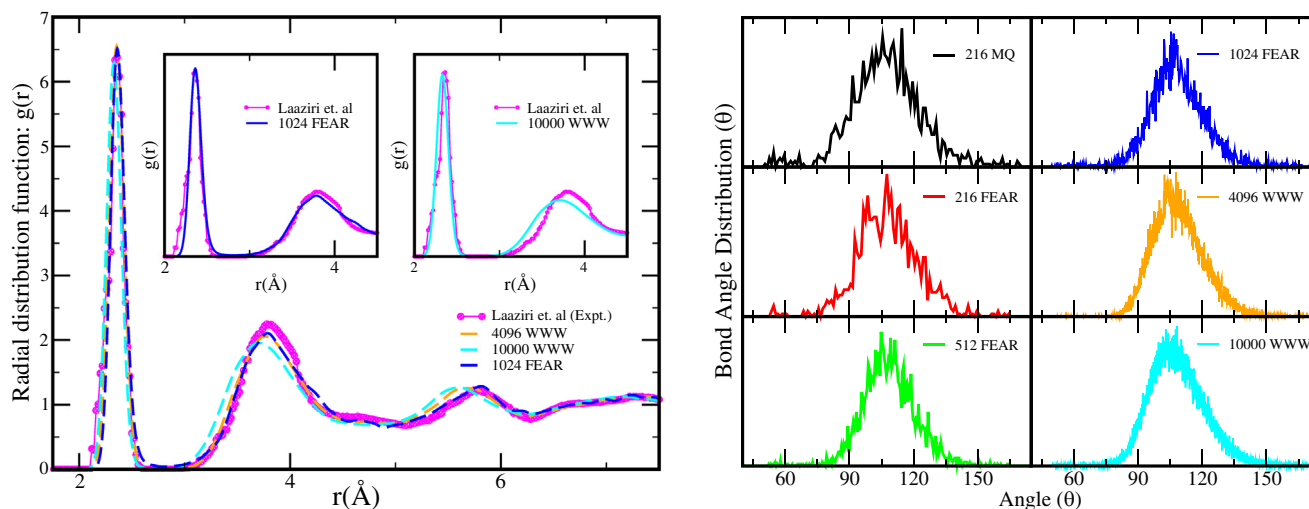


Fig. 2. (left panel) Radial distribution function of different models and their comparison with experiment [25], Inset: Plot of  $g(r)$  of 1024 FEAR and 10,000 WWW models with experimental results, (right panel) Plot of bond-angle distribution for the six models.

### 3.3. Vibrational properties

#### 3.3.1. Vibrational density of states

Vibrational density of states (VDOS) provides key information about the local bonding environments in amorphous solids. It is an important calculation to verify credibility of a model [45]. Meanwhile, it is equally challenging to get a good comparison of vibrational properties between theoretical and experimental results. A lot of factors like: model size, completeness of basis set etc. can affect vibrational properties. We have performed ionic-relaxation on our models to attain a local minimum with forces on each atom less than ( $\sim 0.01$  eV/atom) while simultaneously relaxing lattice vectors to zero pressure. This

results in slightly different number density and a non-orthogonal cell but as shown in our earlier work [46], it is crucial to have coordinates well relaxed before evaluating vibrational properties of the models.

We have computed vibrational properties for our four models (216 MQ, 216 FEAR, 512 FEAR and 1024 FEAR) using the dynamical matrix. We displaced each atom in 6-directions ( $\pm x, \pm y, \pm z$ ) with a small displacement of ( $\sim 0.015$  Å). After, each of these small displacement an *ab initio* force calculation was carried out to obtain force constant matrix (see details [47]). The VDOS for amorphous systems with  $N$  number of atoms is defined as,

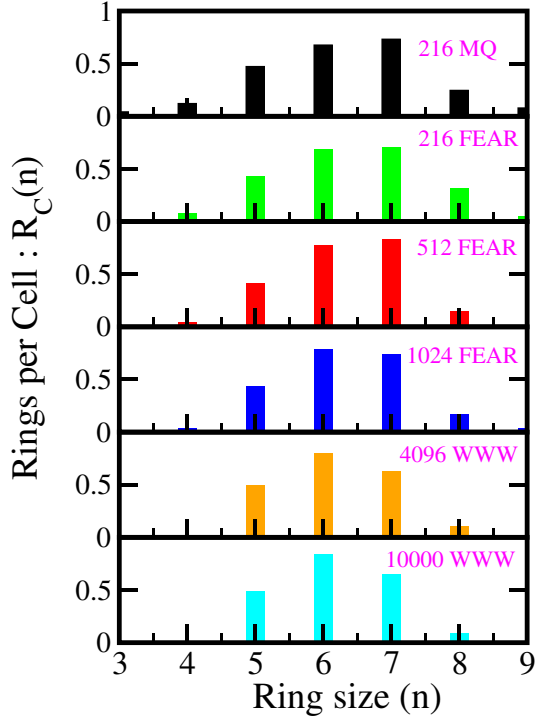


Fig. 3. Rings per cell ( $R_C$ ) for the six models. The ring statistics were obtained using King's method [36] using ISAACS software [37].

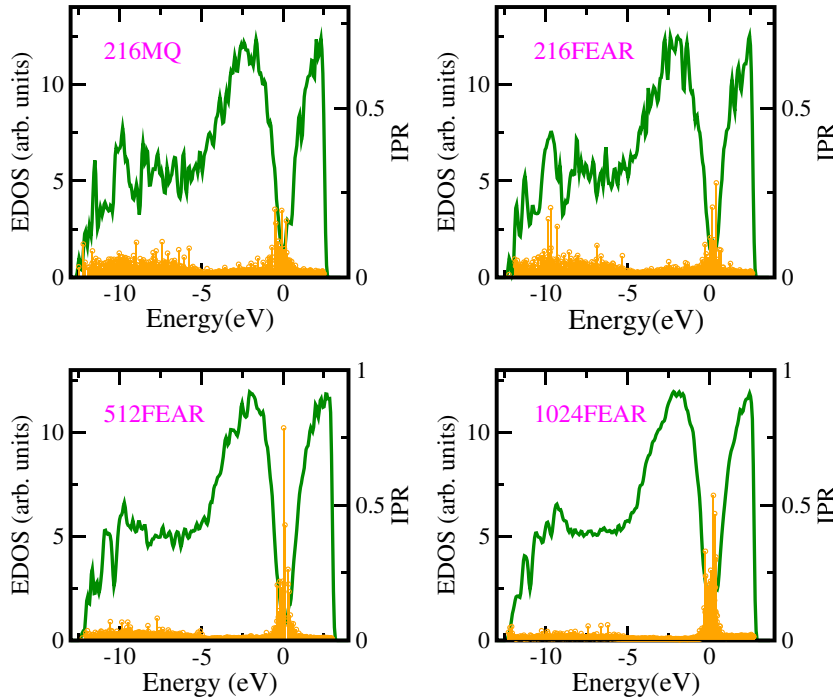


Fig. 4. Plot of Electronic density of states ( $EDOS(E_F = 0)$ ) green-solid lines and Inverse participation ratio (IPR) yellow-drop lines. (For interpretation of the references to color in this figure legend, the reader is referred to the web version of this article.)

$$g(\omega) = \frac{1}{3N} \sum_{i=1}^{3N} \delta(\omega - \omega_i). \quad (1)$$

We have computed the VDOS for our models using the method of Gaussian broadening with a standard deviation of  $\sigma = 1.86$  meV or  $15.0$   $\text{cm}^{-1}$ . The first three zero frequency modes are due to supercell translations, and have been neglected during our calculations of VDOS

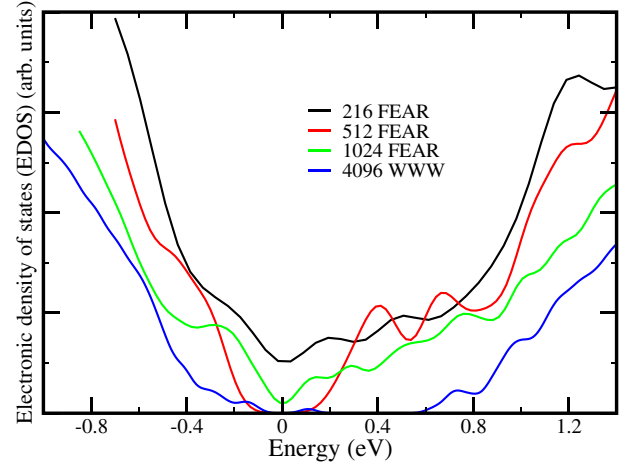
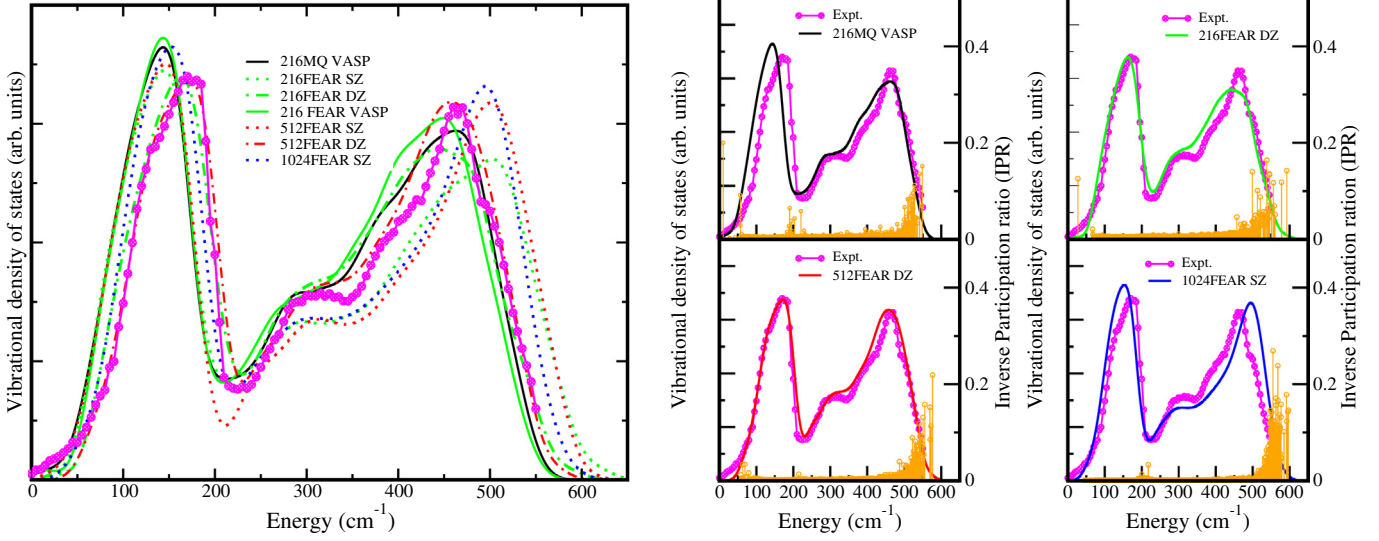


Fig. 5. Comparison of Electronic density of states ( $E_F = 0$ ) of different models obtained by SIESTA with single- $\zeta$  basis set with Harris functional.

and vibrational IPR. We report the VDOS for our different models in Fig. 6.

As seen in Fig. 6, there is a slight horizontal shift in VDOS depending upon system size and completeness of basis set. VDOS calculated with minimal basis set (single- $\zeta$ , SZ) in SIESTA has a qualitative agreement with the experimental result, while slight shift is observed at both low and high energies w.r.t. the experiment. This result is refined by using a more complete basis-set (double- $\zeta$ , DZ), which gives us a better agree-

ment of our models with the experiment. We have computed VDOS using DZ for two of our models (FEAR 216 and FEAR 512). The VDOS obtained for FEAR 512 is strikingly similar to the experiment (Fig. 6, right panel). This switch from minimal basis to double  $\zeta$  basis impacts computation time needed for these calculations and with our resources in hand we simply could not perform a DZ calculations for our FEAR 1024 atom system.



**Fig. 6.** (left panel) Vibrational density of states (VDOS) obtained for different models using VASP-LDA, SIESTA-LDA(single- $\zeta$ , SZ) and SIESTA-LDA (double- $\zeta$ , DZ), (right panel) Comparison of vibrational density of states (VDOS) with experimental results [44] (Note the almost perfect agreement for the 512 DZ calculation). The yellow drop-lines shows Inverse participation ratio (IPR), IPR measures localization of Eigen modes.(For interpretation of the references to color in this figure legend, the reader is referred to the web version of this article.)

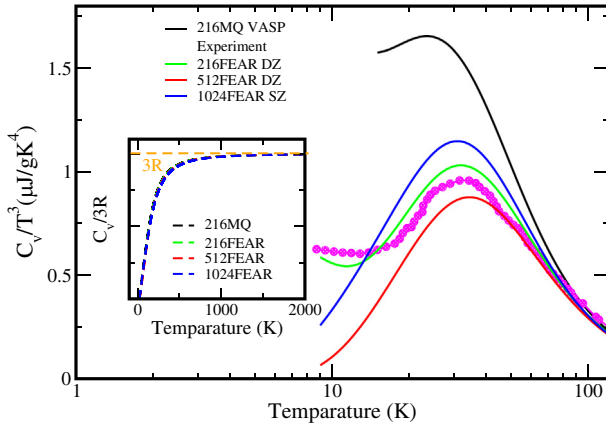


**Fig. 7.** Plot of specific-heat ( $C_V/T^3$ ) for the four models compared with the experimental results [49]. The inset shows the classical (*Dulong-petit*) limit at higher temperature.

**Table 2**

Details of densities obtained after zeropressure relaxation of FEAR models for single- $\zeta$  (SZ) and double- $\zeta$ (DZ) basis sets in SIESTA. Our density for zero pressure (DZ) is closer to the experimental density [48] at 2.28 g/cm<sup>3</sup>.

Models	Volume( $\text{\AA}^3$ )	N(atom/ $\text{\AA}^3$ )	$\rho(\text{g}/\text{cm}^3)$
216 FEAR(SZ)	4643.77	0.046514	2.16
512 FEAR(SZ)	10997.33	0.046557	2.17
1024 FEAR(SZ)	21755.17	0.047067	2.19
216 FEAR (DZ)	4510.57	0.047887	2.23
512 FEAR(DZ)	10652.76	0.048062	2.24
1024 FEAR(DZ)	21213.92	0.048270	2.25

Thus, we can infer completeness of basis-set affects these low energy excitation of atoms in amorphous silicon. The most remarkable feature is the improvement at high frequencies. Based on our zero pressure (double- $\zeta$ , DZ) calculation, it's agreement with experimental VDOS and specific heat (Fig. 7), we predict new density for  $\alpha$ -Si. Our predicted results are tabulated in Table 2 and our results for the zero pressure (double- $\zeta$ , DZ) calculation is close to the experimentally predicted density for  $\alpha$ -Si (2.28 g/cm<sup>3</sup>) [48].

Structural disorder in amorphous solids leads to localized modes and these localized modes can be evaluated by defining a quantity, the inverse participation ratio (IPR). Similar to electronic IPR, we can evaluate vibrational IPR using the obtained normalized displacement vectors. The IPR can be readily evaluated with the obtained normalized displacement vectors ( $u_i^j$ ),  $\mathcal{I}$  for the vibrations can be defined as (for  $j$ th mode),

$$\mathcal{I} = \frac{\sum_{i=1}^N |u_i^j|^4}{\left(\sum_{i=1}^N |u_i^j|^2\right)^2}. \quad (2)$$

The inverse participation ratio value of a localized mode is  $\approx 1$  and for an extended mode is almost equal to zero. We have plotted IPR of our four models in Fig. 6 (right panel). The vibrations at low energies are mostly extended modes, these represent mostly bending type while vibrations at higher energies are dominated by stretching type of modes [46, 47].

### 3.3.2. Specific heat in the harmonic approximation

We evaluate the specific heat in the harmonic approximation using information of vibrational density of states  $g(\omega)$  obtained for our models. We compute the specific heat  $C_V(T)$  from the relation [50]

$$C(T) = 3R \int_0^{E_{\max}} \left(\frac{E}{k_B T}\right)^2 \frac{e^{E/k_B T}}{(e^{E/k_B T} - 1)^2} g(E) dE. \quad (3)$$

Here, the  $g(E)$  is normalized to unity [46, 51]. Our plot for specific heat is shown in Fig. 7. We have a qualitative agreement with the experiment for our four models while the peak around ( $\sim 30$  K) is largely affected by the quality of VDOS obtained. Our three models FEAR-216(DZ), FEAR-512(DZ) and FEAR-1024(SZ) improves the previously agreement of different models with the experiment [49].

We infer from our calculation of VDOS and specific heat that a bigger size model together with a bigger basis set gives us a better understanding of these low energy excitations. This further outlines the importance of our method FEAR, with the resources available to us it is not possible to fabricate melt-quench models of size 512 and 1024 atoms.

## 4. Conclusions

This paper presents an investigation pertaining to the complex

amorphous material (*a*-Si), which was evaluated with respect to its structural, electronic and vibrational properties. Various model types, MQ and FEAR, were constructed of different sizes for this investigation. Our results reveal that the recently developed FEAR method provides an accurate outcome, which correlates quite well with experimental data, even for relatively large structures sizes (512 and 1024). To our knowledge our VDOS result depicts the most clear picture of low energies excitations for *a*-Si. We also predict new density of amorphous silicon based on *ab initio* minimum, our prediction is remarkably close to the experimentally found density.

## Acknowledgments

The authors are thankful to the NSF under grant numbers DMR 1506836, DMR 1507118, DMR 1507166 and DMR 1507670. We would like to thank Dr. Anup Pandey and Dr. Raymond Atta-Fynn for helpful conversations. We also are thankful for the financial support from Condensed Matter and Surface Science (CMSS) at Ohio University. Lastly, We acknowledge computing time provided by the Ohio Supercomputer Center for this research. We also thank NVIDIA Corporation for donating a Tesla K40 GPU which was used in some of these computations.

## References

- [1] R.A. Street (Ed.), vol. 37, Springer-Verlag Berlin Heidelberg, Singapore, 2000.
- [2] B. Djordjevic, M. Thorpe, F. Wooten, Computer model of tetrahedral amorphous diamond, *Phys. Rev. B* 52 (1995) 5685–5689.
- [3] F. Wooten, K. Winer, D. Weaire, Computer generation of structural models of amorphous Si and Ge, *Phys. Rev. Lett.* 54 (1985) 1392–1395.
- [4] G.T. Barkema, N. Mousseau, Event-based relaxation of continuous disordered systems, *Phys. Rev. Lett.* 77 (1996) 4358–4361.
- [5] N. Mousseau, G.T. Barkema, Activated mechanisms in amorphous silicon: an activation-relaxation-technique study, *Phys. Rev. B* 61 (2000) 1898–1906.
- [6] D.A. Drabold, Topics in the theory of amorphous materials, *Eur. Phys. J. B* 68 (2009) 1–21.
- [7] J. Tersoff, Empirical interatomic potential for carbon, with applications to amorphous carbon, *Phys. Rev. Lett.* 61 (1988) 2879–2882.
- [8] N.A. Marks, Generalizing the environment-dependent interaction potential for carbon, *Phys. Rev. B* 63 (2000) 035401.
- [9] R. Car, M. Parrinello, Structural, dynamical, and electronic properties of amorphous silicon: an *ab initio* molecular-dynamics study, *Phys. Rev. Lett.* 60 (1988) 204–207.
- [10] D.A. Drabold, P.A. Fedders, O.F. Sankey, J.D. Dow, Molecular-dynamics simulations of amorphous Si, *Phys. Rev. B* 42 (1990) 5135–5141.
- [11] N. Cooper, C. Goringe, D. McKenzie, Density functional theory modelling of amorphous silicon, *Comput. Mater. Sci.* 17 (1) (2000) 1–6.
- [12] R.L. McGreevy, L. Pusztai, Reverse Monte Carlo simulation: a new technique for the determination of disordered structures, *Mol. Simul.* 1 (1988) 359–367.
- [13] R.L. McGreevy, Reverse Monte Carlo modelling, *J. Phys.: Condens. Matter* 13 (46) (2001) R877.
- [14] D. Keen, R.L. McGreevy, Structural modelling of glasses using reverse Monte Carlo simulation, *Nature* 344 (1990) 423–425.
- [15] P. Biswas, R. Atta-Fynn, D.A. Drabold, Reverse Monte Carlo modeling of amorphous silicon, *Phys. Rev. B* 69 (2004) 195207.
- [16] G. Opletal, T.C. Petersen, A.S. Barnard, S.P. Russo, On reverse Monte Carlo constraints and model reproduction, *J. Comput. Chem.* 38 (2017) 1547–1551.
- [17] M.J. Cliffe, A.P. Bartok, R.N. Kerber, C.P. Grey, G. Csanyi, A.L. Goodwin, Structural simplicity as a restraint on the structure of amorphous silicon, *Phys. Rev. B* 95 (2017) 224108(1–6).
- [18] P. Biswas, R. Atta-Fynn, D.A. Drabold, Experimentally constrained molecular relaxation: the case of hydrogenated amorphous silicon, *Phys. Rev. B* 76 (2007) 125210.
- [19] P. Biswas, D.N. Tafen, D.A. Drabold, Experimentally constrained molecular relaxation: the case of glassy GeSe<sub>2</sub>, *Phys. Rev. B* 71 (2005) 054204.
- [20] B. Meredig, C. Wolverton, A hybrid computational-experimental approach for automated crystal structure solution, *Nat. Mater.* 12 (2012) 123 EP.
- [21] A. Pandey, P. Biswas, D.A. Drabold, Inversion of diffraction data for amorphous materials, *Sci. Rep.* 6 (2016) 33731.
- [22] A. Pandey, P. Biswas, D.A. Drabold, Force-enhanced atomic refinement: structural modeling with interatomic forces in a reverse Monte Carlo approach applied to amorphous Si and SiO<sub>2</sub>, *Phys. Rev. B* 92 (2015) 155205.
- [23] A. Pandey, P. Biswas, B. Bhattarai, D.A. Drabold, Realistic inversion of diffraction data for an amorphous solid: the case of amorphous silicon, *Phys. Rev. B* 94 (2016) 235208.
- [24] B. Bhattarai, A. Pandey, D. Drabold, Evolution of amorphous carbon across densities: an inferential study, *Carbon* (2018), <http://dx.doi.org/10.1016/j.carbon.2018.01.103>.
- [25] K. Laaziri, S. Kycia, S. Roorda, M. Chicoine, J.L. Robertson, J. Wang, S.C. Moss, High resolution radial distribution function of pure amorphous silicon, *Phys. Rev. Lett.* 82 (1999) 3460–3463.
- [26] J. Fortner, J.S. Lannin, Radial distribution functions of amorphous silicon, *Phys. Rev. B* 39 (1989) 5527–5530.
- [27] M.G. Tucker, D.A. Keen, M.T. Dove, A.L. Goodwin, Q. Hui, RMCProfile: reverse Monte Carlo for polycrystalline materials, *J. Phys.: Condens. Matter* 19 (2007) 335218.
- [28] J.M. Soler, E. Artacho, J.D. Gale, A. Garcia, J. Junquera, P. Ordejon, D. Sanchez-Portal, The SIESTA method for *ab initio* order-N materials simulation, *J. Phys.: Condens. Matter* 14 (2002) 2745–2779.
- [29] G. Kresse, J. Furthmüller, Efficient iterative schemes for *ab initio* total-energy calculations using a plane-wave basis set, *Phys. Rev. B* 54 (1996) 11169–11186.
- [30] M. Hacene, A. Anciaux-Sedrakian, X. Rozanska, D. Klahr, T. Guignon, P. Fleurat-Lessard, Accelerating VASP electronic structure calculations using graphic processing units, *J. Comput. Chem.* 33 (32) (2012) 2581–2589.
- [31] M. Hutchinson, M. Widom, VASP on a GPU: application to exact-exchange calculations of the stability of elemental boron, *Comput. Phys. Commun.* 183 (7) (2012) 1422–1426.
- [32] V.L. Deringer, N. Bernstein, A.P. Bartok, M.J. Cliffe, R.N. Kerber, L.E. Marbella, C.P. Grey, S.R. Elliott, G. Csanyi, Realistic Atomistic Structure of Amorphous Silicon from Machine-Learning-Driven Molecular Dynamics, (2018) arXiv:1803.02802.
- [33] K. Jarolimek, R.A. de Groot, G.A. de Wijs, M. Zeman, First-principles study of hydrogenated amorphous silicon, *Phys. Rev. B* 79 (2009) 155206.
- [34] R. Atta-Fynn, P. Biswas, Nearly Defect-free Dynamical Models of Disordered Solids: The Case of Amorphous Silicon, (2018) arXiv:1803.05133.
- [35] G. Opletal, T. Petersen, B. Omalley, I. Snook, D.G. McCulloch, N.A. Marks, I. Yarovsky, Hybrid approach for generating realistic amorphous carbon structure using metropolis and reverse Monte Carlo, *Mol. Sim.* 28 (2002) 927–938.
- [36] S. King, *Nature* 213 (1967) 1112.
- [37] S. Roux, V. Petkov, ISAACS — interactive structure analysis of amorphous and crystalline systems, *J. Appl. Cryst.* 43 (2010) 181–185.
- [38] K. Prasai, P. Biswas, D.A. Drabold, Electronically designed amorphous carbon and silicon, *Phys. Status Solidi A* 213 (2016) 1653–1660.
- [39] J.H. Los, T.D. Kühne, Inverse simulated annealing for the determination of amorphous structures, *Phys. Rev. B* 87 (2013) 214202.
- [40] Y. Pan, F. Inam, M. Zhang, D.A. Drabold, Atomistic origin of Urbach tails in amorphous silicon, *Phys. Rev. Lett.* 100 (2008) 206403.
- [41] D.A. Drabold, Y. Li, B. Cai, M. Zhang, Urbach tails of amorphous silicon, *Phys. Rev. B* 83 (2011) 045201.
- [42] Y. Pan, M. Zhang, D. Drabold, Topological and topological-electronic correlations in amorphous silicon, *Journal of Non-Crystalline Solids* 354 (29) (2008) 3480–3485.
- [43] P.A. Fedders, D.A. Drabold, S. Nakhmanson, Theoretical study on the nature of band-tail states in amorphous Si, *Phys. Rev. B* 58 (1998) 15624–15631.
- [44] W.A. Kamitakahara, C.M. Soukoulis, H.R. Shanks, U. Buchenau, G.S. Grest, Vibrational spectrum of amorphous silicon: experiment and computer simulation, *Phys. Rev. B* 36 (1987) 6539–6542.
- [45] G.P. Lopinski, V.I. Merkulov, J.S. Lanin, Vibrational states of tetrahedral amorphous carbon, *Appl. Phys. Lett.* 69 (1996) 3348–3350.
- [46] B. Bhattarai, D.A. Drabold, Amorphous carbon at low densities: an *ab initio* study, *Carbon* 115 (2017) 532–538.
- [47] B. Bhattarai, D.A. Drabold, Vibrations in amorphous silica, *J. Non-Cryst. Solids* 439 (2016) 6–14.
- [48] J.S. Custer, M.O. Thompson, D.C. Jacobson, J.M. Poate, S. Roorda, W.C. Sinke, F. Spaepen, Density of amorphous Si, *Appl. Phys. Lett.* 64 (4) (1994) 437–439.
- [49] B.L. Zink, R. Pietri, F. Hellman, Thermal conductivity and specific heat of thin-film amorphous silicon, *Phys. Rev. Lett.* 96 (2006) 055902.
- [50] A. Maradudin, E. Montroll, G.H. Weiss, *Theory of Lattice Dynamics in the Harmonic Approximation*, Academic Press, New York, 1963, p. 123.
- [51] S.M. Nakhmanson, D.A. Drabold, Low-temperature anomalous specific heat without tunneling modes: a simulation for *a*-Si with voids, *Phys. Rev. B* 61 (2000) 5376–5380.